Synthesis and Disassembly of an Organometallic Polymer Comprising Redox Active Co_4S_4 Clusters and Janus Biscarbene Linkers

Jonathan H. Gillen,[a] Connor A. Moore,[a] My Vuong,[a] Juvairia Shajahan,[b] Mitchell R. Anstey,[c]

Jeffery R. Alston,[b] and Christopher M. Bejger[a]*

[a]Department of Chemistry, The University of North Carolina at Charlotte, Charlotte, North Carolina 28223, United States

[b]The Joint School of Nanoscience and Nanoengineering, North Carolina A&T State University, Greensboro, NC 27401, United States

[c]Department of Chemistry, Davidson College, Davidson, NC 28035, United States

Supporting Information

I. Chemicals, Synthetic Details, & General Information

All manipulations were performed under an inert atmosphere of dry N_2 using a Schlenk line or MBraun UniLab Pro glovebox unless otherwise noted. Tetrahydrofuran (THF), toluene, dichloromethane (DCM), hexane, and diethyl ether were purged with N_2 and dried on an MB-SPS solvent purification system from MBraun. Acetonitrile anhydrous (99.8%, Aldrich), benzene anhydrous (Drisolve), 1,4-dioxane anhydrous (99.8%, Alfa Aesar) were freeze pump thawed 3-4x. NaH 60% in mineral oil (Aldrich) for imidazolium deprotonation was washed thoroughly over a medium filter with hexane under a N_2 atmosphere and pumped dry. All other chemicals were purchased from commercial sources and used as received, including N,N-dimethylformamide anhydrous/under argon (99.8%, Alfa Aesar), 1,2,4,5 benzene tetrahydrochloride (95%, Aldrich), formic acid (96%, Alfa Aesar), hydrochloric acid (Macron Fine Chemicals), 2-bromopropane (99%, TCI), bromoethane (98% Alfa Aesar), sodium carbonate monohydrate (99.5%, Alfa Aesar), anhydrous potassium carbonate (99%, EMD), benzimidazole (98%, Acros Organics), cobalt (II) chloride anhydrous (99.7%, Alfa Aesar), triisopropylphosphine (98%, Alfa Aesar), bis(trimethylsilyl)-sulfide (95%, Acros Organics), KO*t*Bu (potassium tert-butoxide, 98%, Aldrich), and potassium chunks in mineral oil (98%, Alfa Aesar).

Synthesis of 1,3-Dihydro-1,3-bisisopropyl-2H-benzimidazol-2-ylidene (Pr^i_2NHCBz) (3). The free carbene was prepared using a modified literature prep.[1] KO*t*Bu (208 mg, 1.85 mmol) was placed in a 20 mL vial inside the glovebox and dissolved in THF (6 mL). 1,3-Diisopropylbenzimidazolium bromide[2] (526 mg, 1.85 mmol) was added to the vial and the suspension was stirred for one day at room temperature. The suspension was filtered to yield a yellow liquid, which was dried in vacuo to give free carbene **3** as an off-white solid. Yield 333 mg (88%).

Synthesis of biscarbene 4. 1,1′,3,3-Tetra-isopropyl-5,5′-bibenzimidazolium bromide was first prepared following a modified procedure.[44] Briefly, the reported prep yielded a product with an 85% purity (as measured via ^{1}H-NMR). The reaction was repeated three times on the resulting product of precursory reactions to achieve a 98% purity of an overall 25% yield. All solid product was washed with chloroform to remove any dimethyl amine that formed during the reaction. The free biscarbene was then prepared following a modified procedure by Bielawski and coworkers.[45] The imidazolium dibromide (100 mg, 0.20 mmol), NaH (12.2 mg, 0.51 mmol), and KO*t*Bu (2 mg, 18 µmol) were suspended in THF or benzene (5 mL) and stirred for 2 days. The resulting suspension was syringe filtered and dried in vacuo producing a yellow/tan solid product. A concentrated solution of the biscarbene in THF layered with hexanes produced X-ray quality single crystals. Yield: 25mg (37%). *(Note: freeze drying from benzene produces a yellow cotton candy like solid)*. ^{1}H NMR (500 MHz, C_6D_6) δ 7.00 (2 H, s), 4.48 (4 H, sept), 1.65 (24 H, d) ppm. ^{13}C NMR (125 MHz, C_6D_6) δ 225.07, 131.81, 90.06, 49.51, 23.46 ppm.

Synthesis of $Co_4S_4(Pr^i_2NHCBz)_4$ (2). $Co_4S_4(P^iPr_3)$ (**1**) (251 mg, 0.25 mmol) and Pr^i_2NHCBz (**3**) (253 mg, 1.5 mmol) were placed in a 25 mL Schlenk flask and dissolved in THF (10 mL). The dark yellow-green solution was stirred at 60 °C under an N_2 atmosphere for two days and then refluxed at 78 °C for an additional two days. The resulting dark red solution was dried in vacuo, concentrated in ether (2mL), syringe-filtered, and placed in a 20 mL vial. After three days sealed and undisturbed, X-ray quality crystals formed and were gently washed with chilled ether (4 x 3 mL). Yield: 296 mg (quant.) (single crystal yield 30%). ^{1}H NMR (500 MHz, C_6D_6) δ 12.54 (12 H, s (br)), 6.66 (2H, s), 6.45 (2H, s) ppm. Anal. Calc. for $Co_4S_4N_8C_{52}H_{72}$: C 53.93%, H 6.63%, N 8.98%. Found: C 49.60%, H 6.22%, N 8.58%.

Synthesis of Co_4S_4-MCOP. Cluster **1** (30.8 mg, 0.0306 mmol) and biscarbene **4** (25.0 mg, 0.0766 mmol) were weighed into two, separate 20 mL vials and each dissolved in benzene (2.5 mL). The solutions were then transferred and mixed into a 15 mL Chemglass pressure vessel and sealed under a N_2 atmosphere. The vessel was placed in an oven at 100 °C. After 2-5 days the resulting purple solid was separated by centrifugation and washed with THF (6 × 1 mL) inside the glovebox. Subsequent drying under vacuum produced a black solid with substantially less volume. Yield: 14 mg (45%). The reaction has also been repeated using toluene, dioxane, and THF with similar yields/products (~20-50%).

We also prepared a less sterically hindered tetrakis-N-ethyl-biscarbene in order to probe the steric effect of the linker on crystallinity. Polymers were synthesized using this smaller linker under the same conditions listed above. The Co_4S_4-MCOP-ET solids were similar in color, morphology, and composition via SEM and EDS. Structurally, the PXRD pattern of this ethyl analog did not differ from that of Co_4S_4-MCOP. Fabricated electrodes using the polymer made with tetrakis-N-ethyl-biscarbene linkers exhibit one oxidation at a similar potential. See **Section XIII** below for PXRD, SEM, EDS, and CV of this derivative.

Depolymerization of Co_4S_4-MCOP. A suspension of polymer (13.8 mg) in deuterated benzene (1.2 mL) was mixed with a solution of free carbene $Pr^i{}_2NHCMe_2$ (48 mg, ~20 equiv., 1.2 mL) in a 2-dram vial. The solution was stirred for two days inside the glovebox on a hotplate at 50 ^oC. During this time, the majority of the solid dissolved and the solution turned dark, reddish brown. The solution was allowed to sit for several hours before an aliquot (1 mL) was taken from the top of the reaction mixture and analyzed by NMR.

Characterization

Nuclear Magnetic Resonance (NMR) Spectroscopy

NMR spectra were obtained on a Jeol ECA-500 NMR for ^{1}H (500 MHz), ^{13}C (125 MHz), and ^{31}P (202 MHz). NMR tubes were prepared using deuterated solvents purchased from Cambridge Isotope Laboratories >95% and sealed by parafilm or a J-Young needle valve.

Thermogravimetric Analysis (TGA)

Thermogravimetric analysis was performed on vacuum dried solid in a platinum pan using a Mettler Toledo TGA/SDTA851e supplied by compressed N_2.

Electrochemistry

All electrochemical measurements were obtained on a Gamry 1000E potentiostat and were recorded on Gamry Framework Software (Version 7.02). Analysis of the data was done using

Gamry Echem Analyst (Version 7.02). Measurements were performed with a three-electrode setup with a working glassy carbon electrode (3.0 mm), a platinum wire counter electrode, and a platinum wire as a pseudo-reference electrode. The solid polymer was physically absorbed onto the surface of the glassy carbon electrode while still wet with THF. Approximately 2 mg of wet polymer covering ½ of the surface of the GCE were loaded for each measurement. All measurements were collected inside the glovebox under a dinitrogen atmosphere. Ferrocene was used post analytically to reference voltages. CV scans taken with modified electrodes did not exhibit redox activity when the adsorbed solid is physically removed. Additionally, no oxidation or reduction events could be measured (with a clean working electrode) in the residual solution after the polymer-modified electrode had been submerged for an hour.

Electronic Absorption Spectroscopy

A Cary 300 Bio UV-Visible Spectrometer running Scan v1.00(6) was used to collect the UV-vis spectra with solutions of THF inside of sealed quartz cuvettes to maintain an air free atmosphere. The dried polymer was run as a powdered solid, sealed between two slides, and suspended in bSi-201 quick cure epoxy to prevent oxidation.

Scanning Electron Microscopy and Energy Dispersive X-ray Spectroscopy

Scanning electron micrographs were obtained on a JEOL JSM-6460LV SEM instrument using a 5-15kV accelerating voltage while collecting data through the SEM Control User Interface (Version 6.21). Energy dispersive X-ray spectrographs were taken using the built in EDAX and worked up using the APEX software. SEM samples were pumped down and placed on a copper or carbon tape background with a 60 second air exposure while being loaded. During this exposure, samples would occasionally produce smoke from an exothermic reaction.

Single Crystal X-ray Diffraction

Single Crystal X-ray diffraction was performed using an Oxford Diffraction Gemini A Ultra SCXRD. Samples were dried for 30 min by vacuum and suspended in Nujol mineral oil before being transferred to the sampling stage and mounted on loops.

X-ray Photoelectron Spectroscopy

X-ray Photoelectron Spectroscopy was collected using a Thermo Scientific ESCALAB Xi with a twin crystal monochromatic Al Kα source (500 µm), and a pass energy of 20.0 eV, with a spot size of 200 µm. Samples were stored in an inert atmosphere and transferred rapidly to the loading chamber of the XPS after mounting the sample. To prevent charging of the surface, all samples were probed in the presence of a low energy electron flood gun. Charging can lead to shifting and distortion of the XPS spectra, so a low energy electron flood gun was used to limit charging.

Powder X-ray Diffraction

Powder X-ray diffraction patterns were obtained from 11-BM APS Synchrotron Beamline (Bending Magnet Source) at the Argonne National Laboratory (Lemont, Il, USA). X-ray samples were pumped dry, ground by mortar and pestle, and packed into a 1.105 mm outer diameter, 0.1 mm wall Kapton capillary inside a nitrogen glovebox. The capillary ends were then sealed with bSi-201 quick cure epoxy and allowed to cure for at least 24 hours.

High resolution synchrotron powder diffraction data were collected using beamline 11- BM at the Advanced Photon Source (APS), Argonne National Laboratory using an average wavelength of λ = 0.4581 Å. Discrete detectors covering an angular range from 0.5 to 50° 2θ, with data points collected every 0.001° 2θ and scan speed of 0.01°/s. The predicted structure was generated by forming a diamond cubic crystal structure with each Co_4S_4 unit representing a single lattice point and a lattice constant of a = 29.56 Å as based upon the SCXRD data for the free carbene and model cluster. It should be noted that this structure omits the alkyl groups and assumes a carbene-cobalt bond length and core geometry as found in the model cluster.

Surface Area Analysis

Surface area was estimated by BET isotherms using a Quantachrome Instruments NOVA 2200e Surface Area & Pore Size Analyzer supplied by compressed N_2. Samples were pumped dry for 24 hours with a potential air exposure while the BET tube was being transferred to the degassing line.

II. Single Crystal X-ray Diffraction Figures

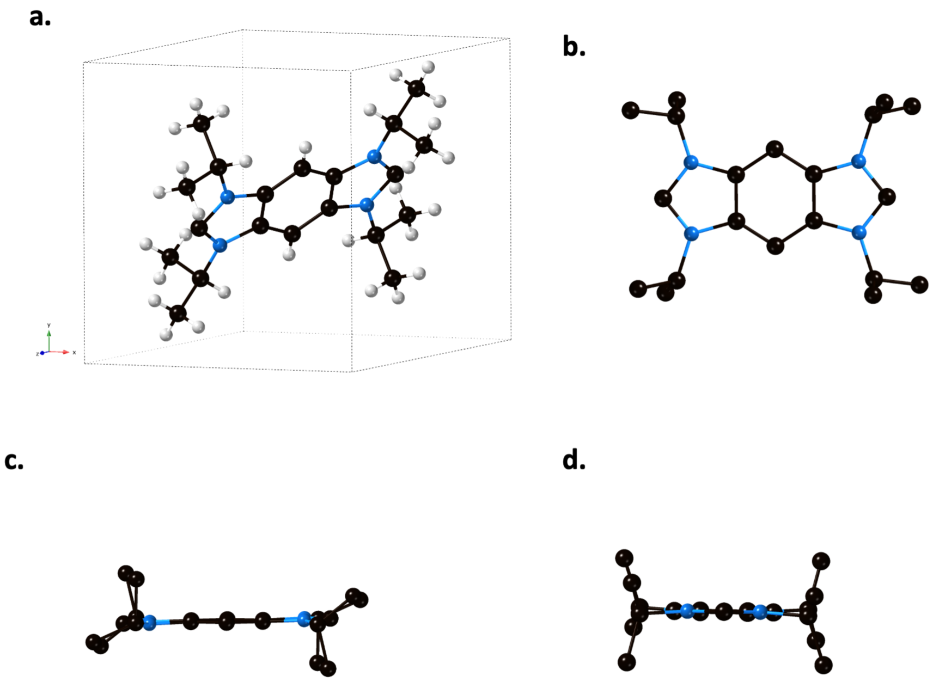

Figure S1. Single crystal X-ray structure of **4** depicted as ball-and-stick. (a) unit cell; (b) top view; (c) side view; (d) front view looking down C_{NHC}. Nitrogen, light blue; carbon, black; hydrogen, white.

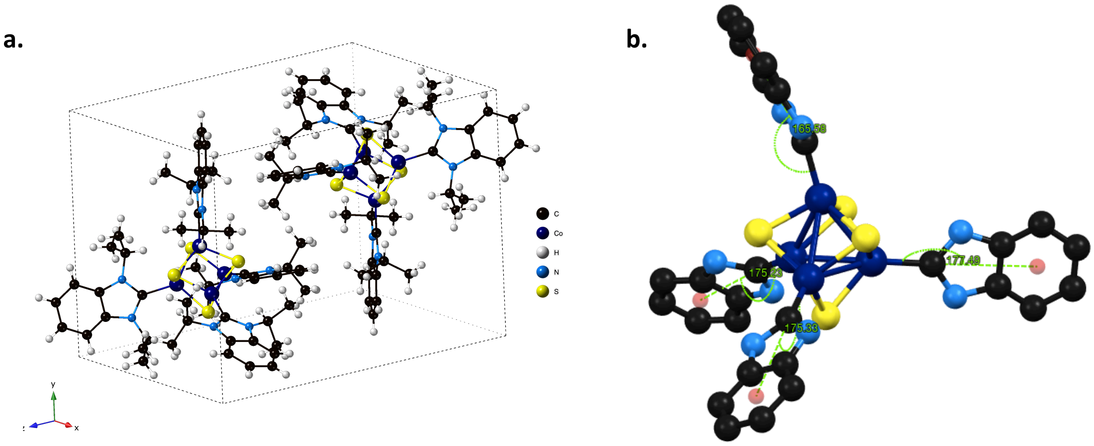

Figure S2. Single crystal X-ray structure of **2** depicted as ball-and-stick. (a) unit cell; (b) view depicting the bent, nonlinear (166°) connection of the top Co-C_{NHC} bond with isopropyl groups and hydrogen atoms omitted. Cobalt, dark blue; sulfur, yellow; nitrogen, light blue; carbon, black; hydrogen, white.

III. Scanning Electron Micrographs & Energy Dispersive X-ray Spectroscopy Scans

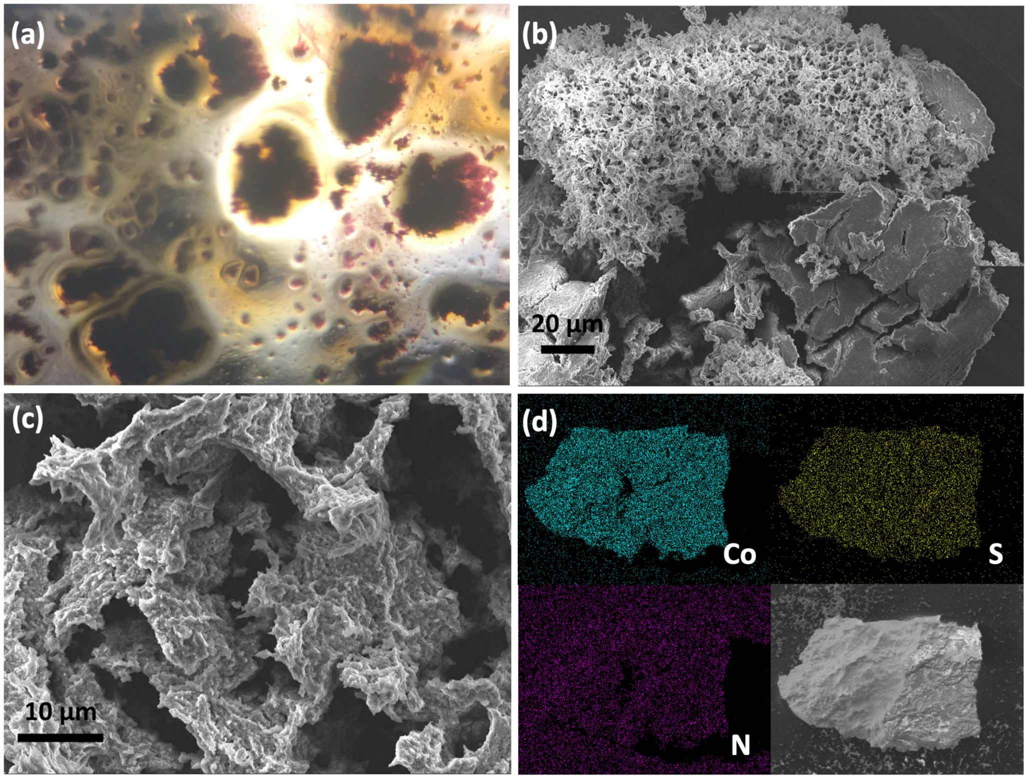

Figure S3. (a) Microscope image of Co_4S_4-MCOP at 30X magnification; (b) and (c) SEM micrographs of Co_4S_4-MCOP; and (d) EDS analysis mapping of Co_4S_4-MCOP (teal: cobalt; yellow: sulfur; purple: nitrogen).

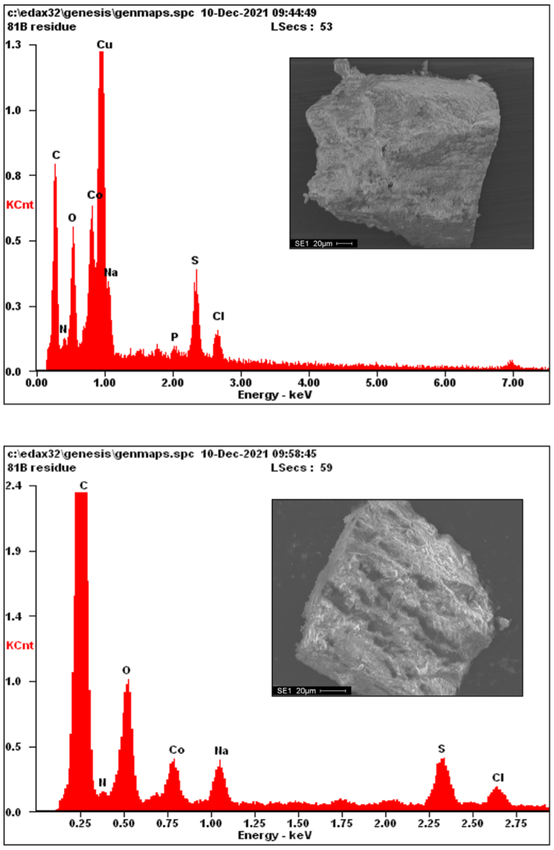

Element	Wt%	At%
CK	28.55	57.66
NK	02.22	03.85
OK	05.78	08.76
CoL	11.12	04.58
CuL	40.35	15.40
NaK	02.92	03.08
PK	00.70	00.55
SK	05.67	04.29
ClK	02.69	01.84
Matrix	Correction	ZAF

Element	Wt%	At%
CK	65.64	78.09
NK	04.76	04.86
OK	11.93	10.65
CoL	08.68	02.10
NaK	02.17	01.35
SK	04.59	02.05
ClK	02.23	00.90
Matrix	Correction	ZAF

Figure S4. EDS survey scans and elemental composition of Co_4S_4-MCOP. The top spectrum was collected using copper tape as a background and the bottom spectrum was run with the sample placed on carbon tape.

IV. Nuclear Magnetic Resonance Spectroscopy

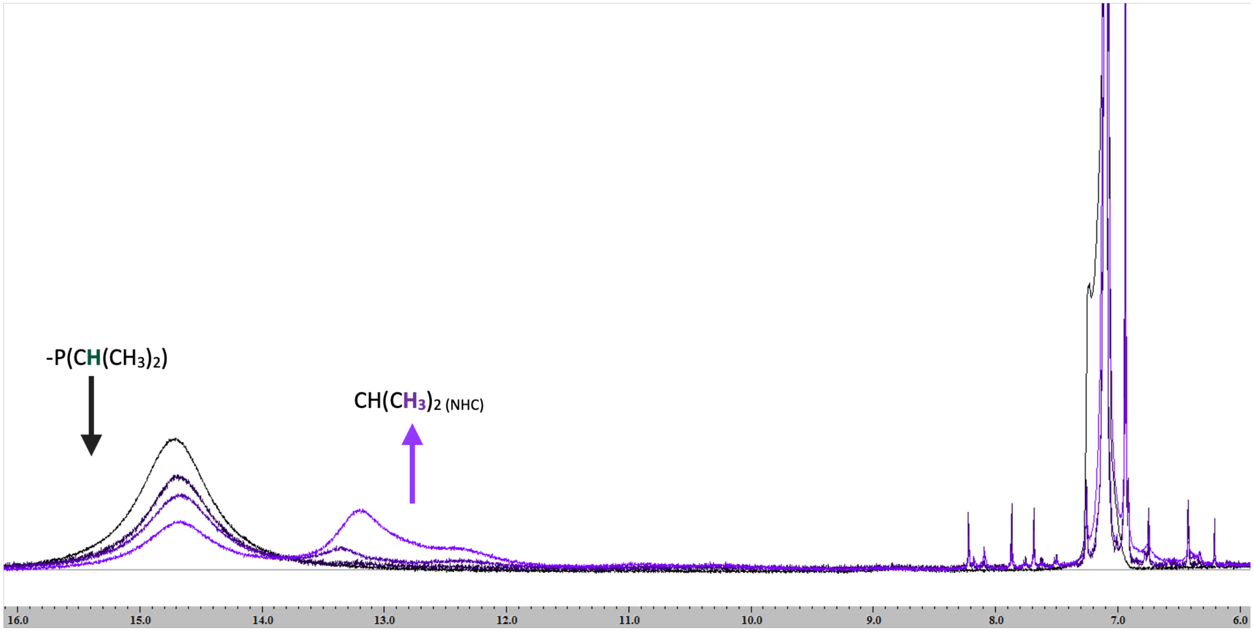

Figure S5. Polymerization reaction monitored via ^{1}H-NMR in C_6D_6. NMR was taken with cluster **1** only (black) then 2.5 equivalents of biscarbene **4** were added and the NMR was collected again after 1 hour, 18 hours, and 72 hours. The same experiment was also run while heating but proceeded too quickly to monitor.

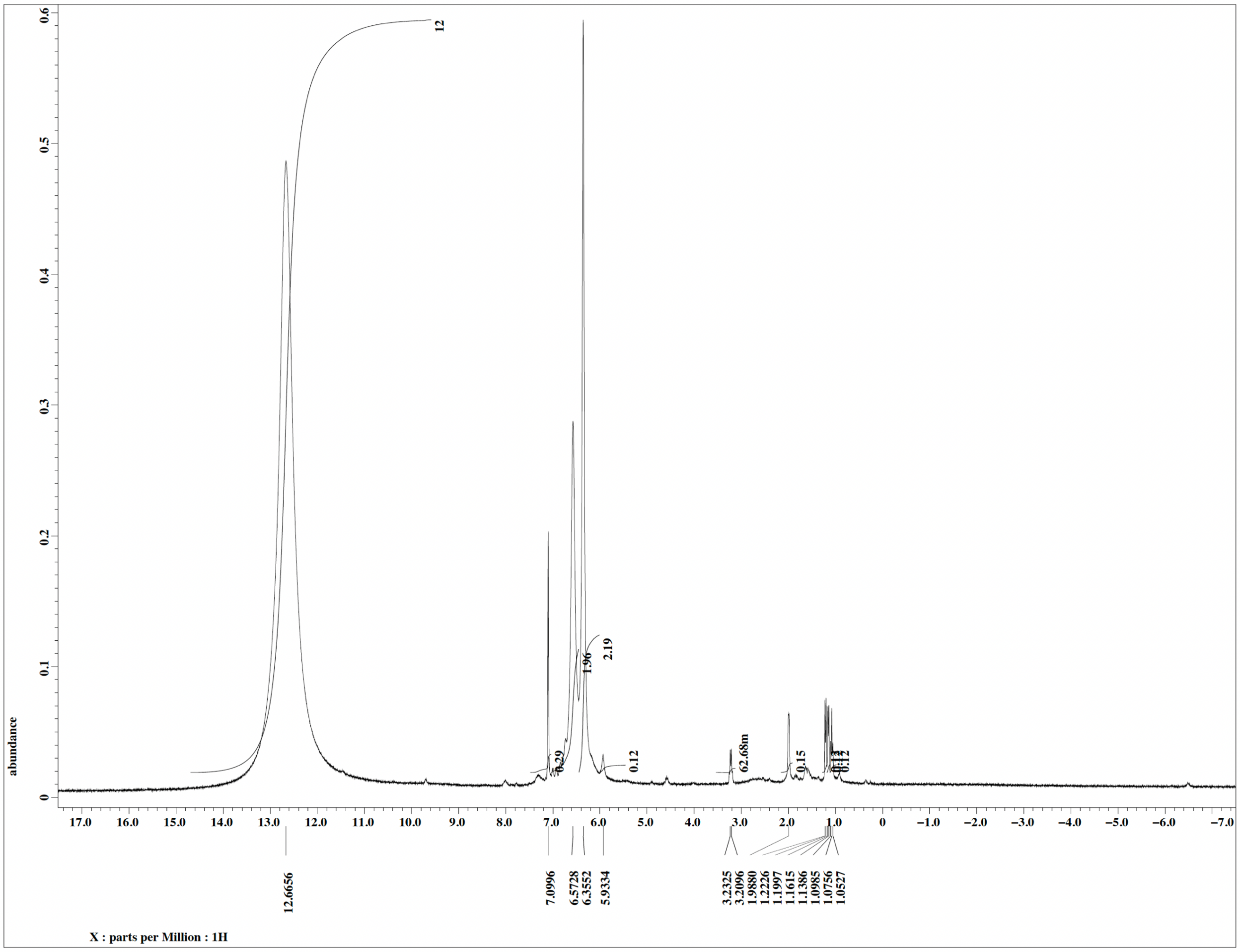

Figure S6. ^{1}H-NMR spectrum of **2** in C_6D_6.

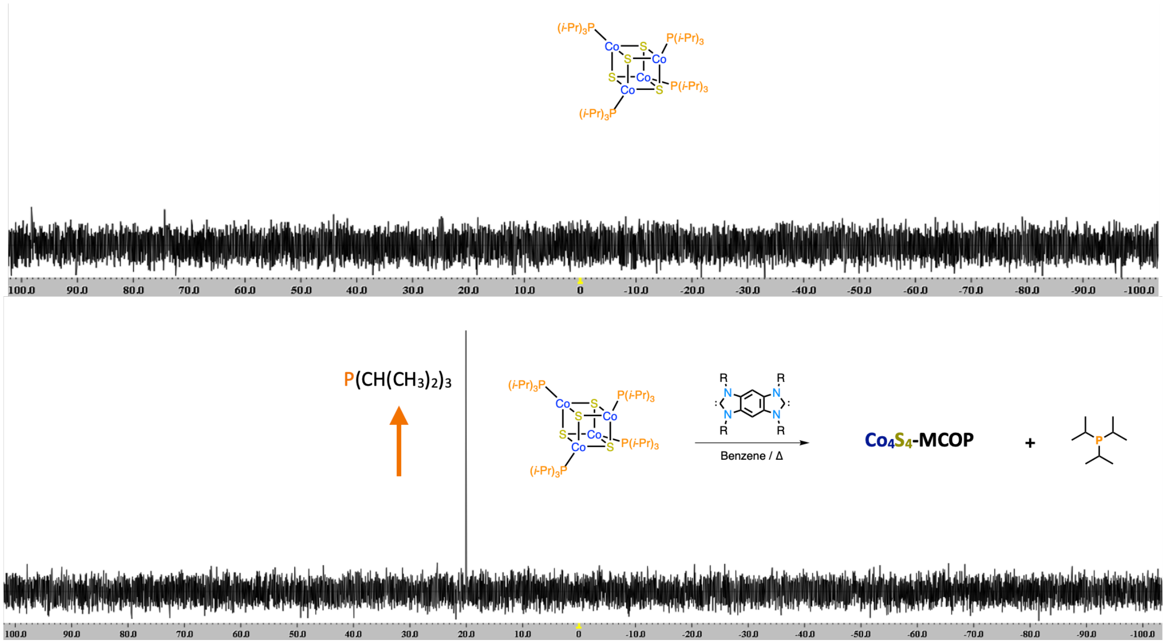

Figure S7. Polymerization reaction monitored via ^{31}P-NMR in C_6D_6. Cluster **1** (top spectrum) and Cluster **1** mixed with two equivalents of biscarbene **4** after heating for one hour (bottom spectrum).

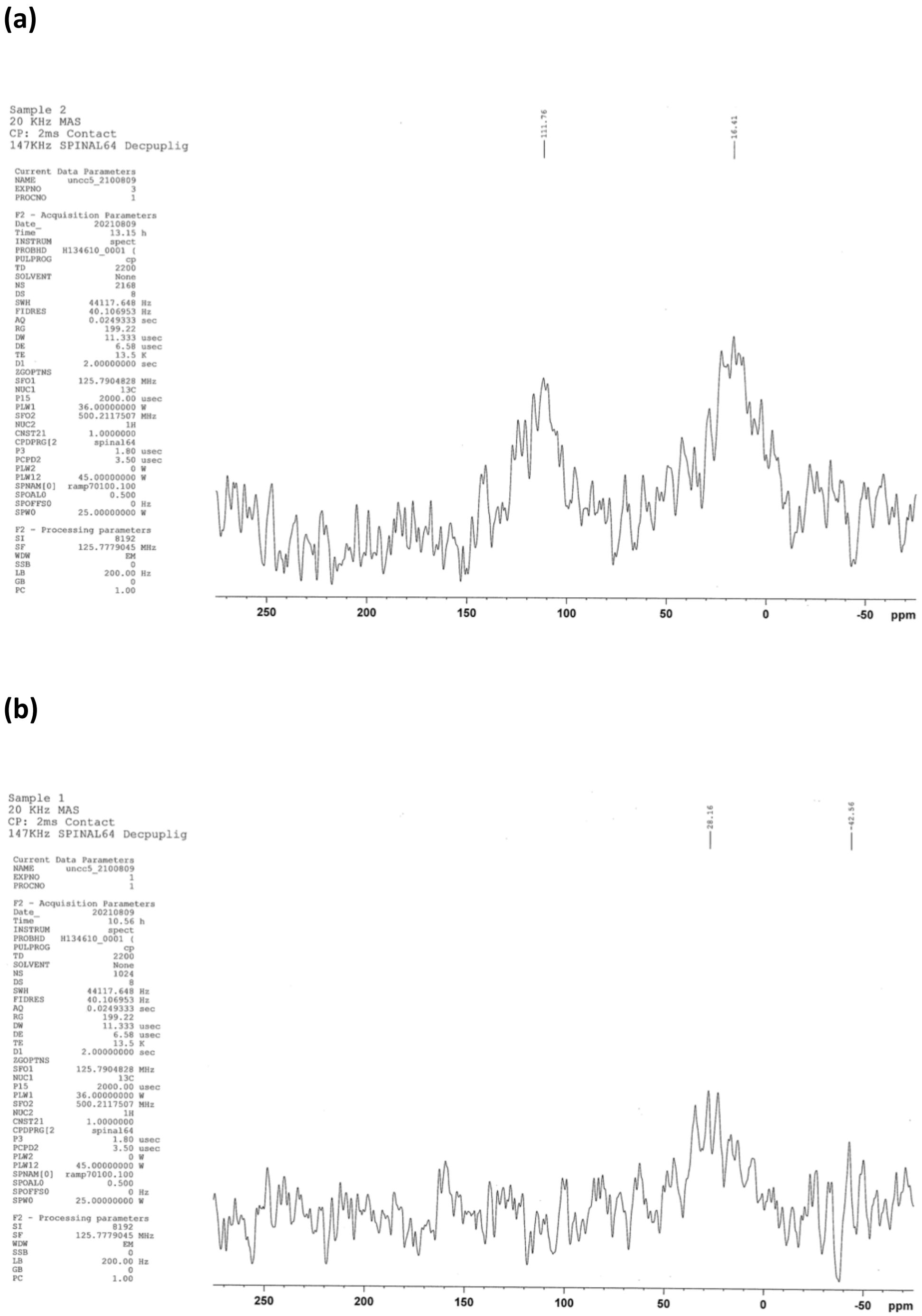

```
Sample 2
20 KHz MAS
CP: 2ms Contact
147KHz SPINAL64 Decpuplig

 Current Data Parameters
 NAME       uncc5_2100809
 EXPNO                  3
 PROCNO                 1

 F2 - Acquisition Parameters
 Date_           20210809
 Time               13.15 h
 INSTRUM            spect
 PROBHD   H134610_0001 (
 PULPROG               cp
 TD                  2200
 SOLVENT             None
 NS                  2168
 DS                     8
 SWH            44117.648 Hz
 FIDRES         40.106953 Hz
 AQ             0.0249333 sec
 RG                199.22
 DW                11.333 usec
 DE                  6.58 usec
 TE                  13.5 K
 D1            2.00000000 sec
 ZGOPTNS
 SFO1         125.7904828 MHz
 NUC1                 13C
 P15              2000.00 usec
 PLW1         36.00000000 W
 SFO2         500.2117507 MHz
 NUC2                  1H
 CNST21         1.0000000
 CPDPRG[2        spinal64
 P3                  1.80 usec
 PCPD2               3.50 usec
 PLW2                   0 W
 PLW12        45.00000000 W
 SPNAM[0]  ramp70100.100
 SPOAL0             0.500
 SPOFFS0                0 Hz
 SPW0         25.00000000 W

 F2 - Processing parameters
 SI                  8192
 SF           125.7779045 MHz
 WDW                   EM
 SSB                    0
 LB                200.00 Hz
 GB                     0
 PC                  1.00
```

```
Sample 1
20 KHz MAS
CP: 2ms Contact
147KHz SPINAL64 Decpuplig

 Current Data Parameters
 NAME       uncc5_2100809
 EXPNO                  1
 PROCNO                 1

 F2 - Acquisition Parameters
 Date_           20210809
 Time               10.56 h
 INSTRUM            spect
 PROBHD   H134610_0001 (
 PULPROG               cp
 TD                  2200
 SOLVENT             None
 NS                  1024
 DS                     8
 SWH            44117.648 Hz
 FIDRES         40.106953 Hz
 AQ             0.0249333 sec
 RG                199.22
 DW                11.333 usec
 DE                  6.58 usec
 TE                  13.5 K
 D1            2.00000000 sec
 ZGOPTNS
 SFO1         125.7904828 MHz
 NUC1                 13C
 P15              2000.00 usec
 PLW1         36.00000000 W
 SFO2         500.2117507 MHz
 NUC2                  1H
 CNST21         1.0000000
 CPDPRG[2        spinal64
 P3                  1.80 usec
 PCPD2               3.50 usec
 PLW2                   0 W
 PLW12        45.00000000 W
 SPNAM[0]  ramp70100.100
 SPOAL0             0.500
 SPOFFS0                0 Hz
 SPW0         25.00000000 W

 F2 - Processing parameters
 SI                  8192
 SF           125.7779045 MHz
 WDW                   EM
 SSB                    0
 LB                200.00 Hz
 GB                     0
 PC                  1.00
```

Figure S8. Solid State CP-MAS ^{13}C-NMR spectra of (a) **2** and (b) Co_4S_4-MCOP. The spectra are unable to be resolved due to the paramagnetic nature of the compounds.

V. Infrared Spectroscopy

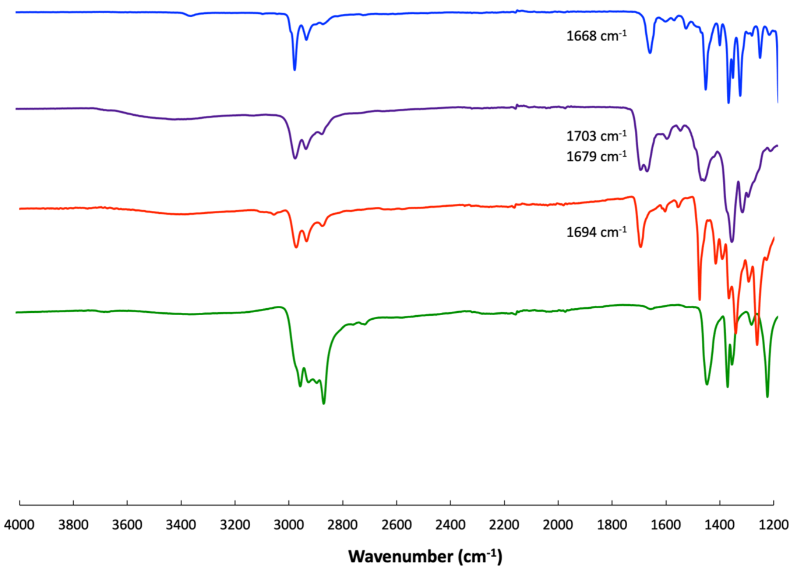

Figure S9. Infrared spectra of **4** (blue), Co_4S_4-MCOP (purple), **2** (red), and **1** (green).

VI. X-ray photoelectron spectroscopy

Thermo Scientific Avantage Data System software was used for the acquisition and processing of the data. Using a smart background, atomic percentages were calculated from the absolute peak intensity signal of each element detected in the survey spectra of each sample. Elements detected in the survey spectra were studied at characteristic binding energies (BE) to assess the intensity (count/second) of each signal. Characteristic binding energies were compared with data from the Thermo Fisher XPS Knowledge Database. Sulphur spectra were collected in a binding energy range of 157-174 eV. Carbon spectra were collected in a binding energy range of 279-294 eV. Nitrogen spectra were collected in a binding energy range of 392-406 eV. Oxygen spectra were collected in a binding energy range of 525 - 534 eV. Cobalt spectra were collected in a binding energy range of 771 - 812 eV. XPS measurements were made at 3 discrete spots on each powdered sample. A slight increase in oxygen percent is expected due to oxidation during transfer, as well as background adventitious carbon is expected due to surface contamination (~285 eV). Reported atomic compositions are calculated from the average of the three spot measurements of each sample.

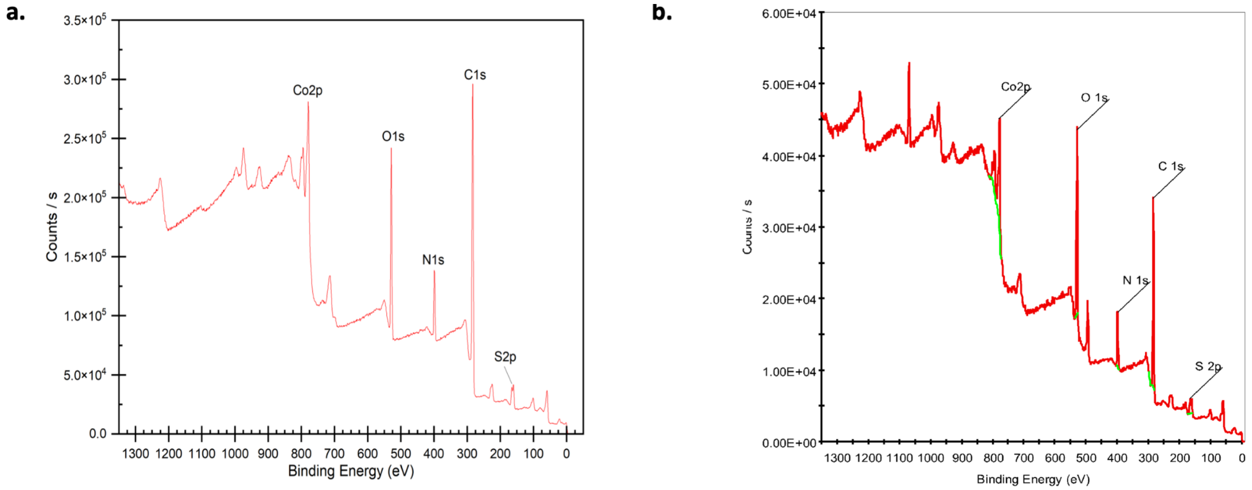

Figure S10. XPS survey spectra of (a) **2** and (b) Co_4S_4-MCOP.

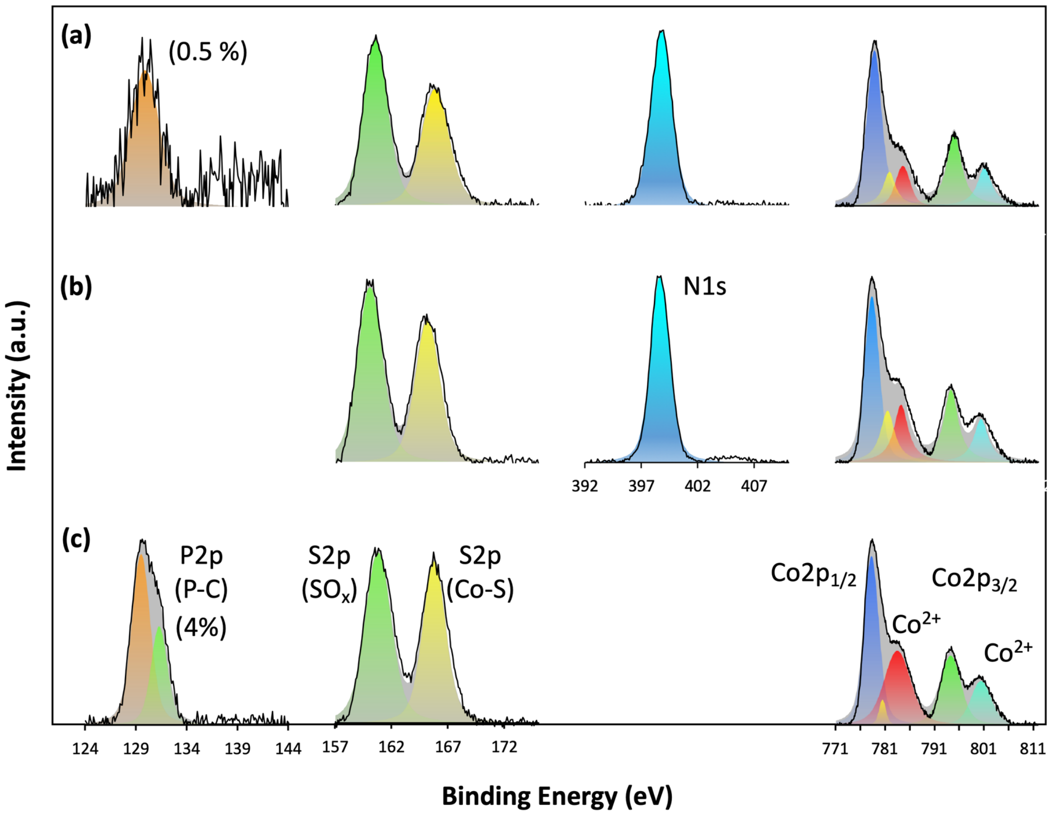

Figure S11. High Resolution X-ray photoelectron spectra of (a) Co_4S_4-MCOP, (b) $[Co_4S_4(Pr^i{}_2NHCBz)_4]$ **2**, and (c) $[Co_4S_4(PPr^i{}_3)_4]$ **1**.

VII. UV-Vis Absorption Spectroscopy

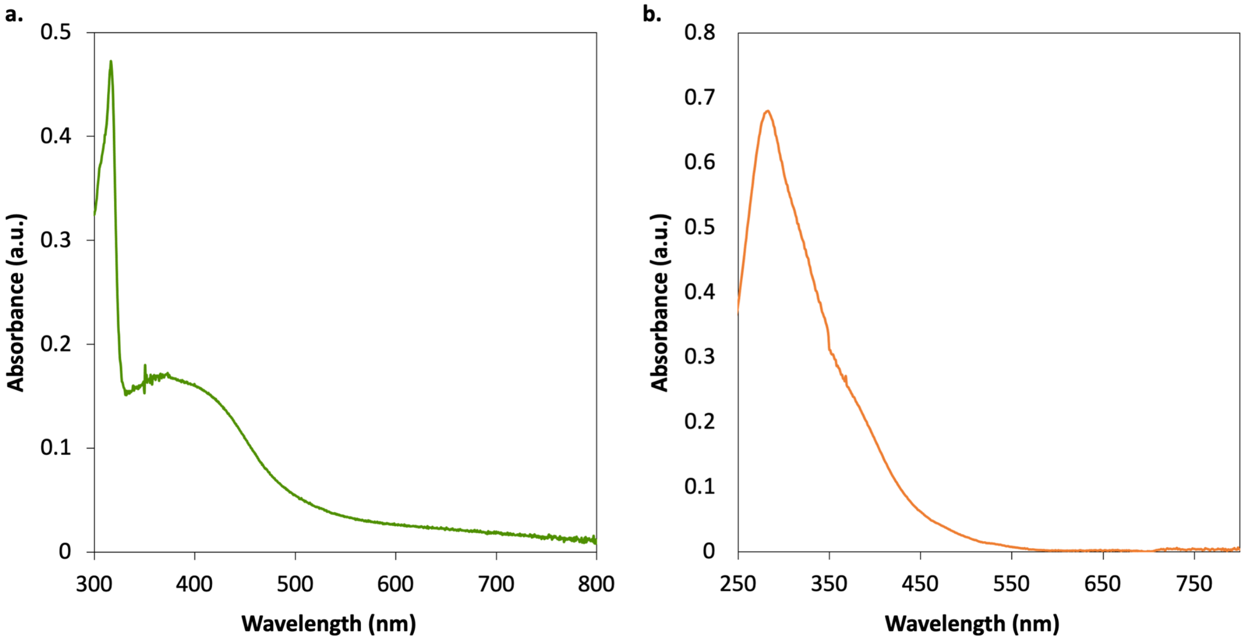

Figure S12. UV-vis absorption spectra of (a) **2** (0.1 mM in THF) and (b) **1** (0.1 mM in THF).

VIII. Surface Area Analysis

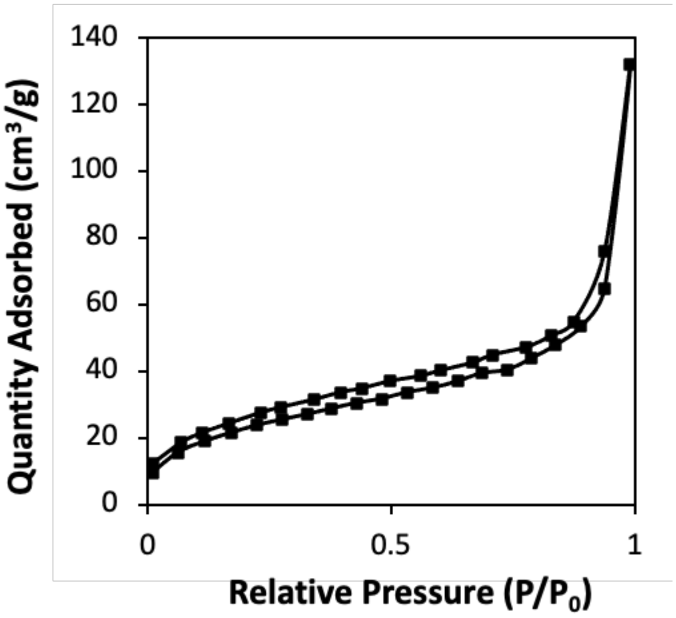

Figure S13. N_2 adsorption and desorption isotherms at 77K of Co_4S_4-MCOP.

IX. Electrochemistry

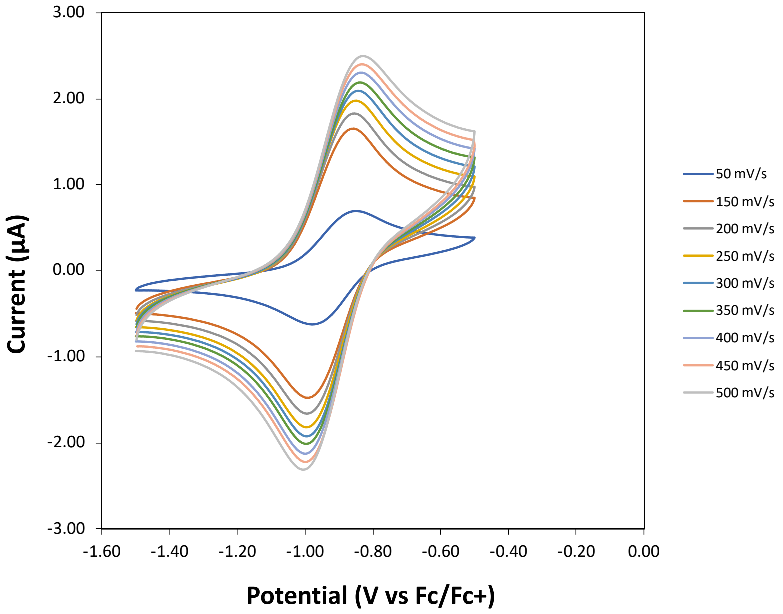

Figure S14. Cyclic voltammograms of Co_4S_4-MCOP modified glassy carbon working electrode at various scan rates. Recorded using a Pt wire counter electrode and Pt pseudo reference electrode in acetonitrile with $TBAPF_6$ as the supporting electrolyte and referenced vs Fc/Fc^+.

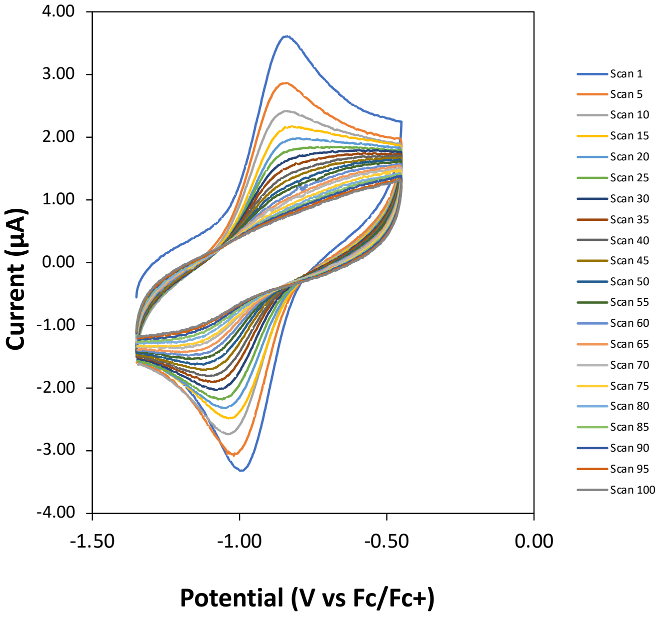

Figure S15. Cyclic voltammograms of Co_4S_4-MCOP modified glassy carbon working electrode scanned at 50 mV/s for 100 sequential scans. Recorded using a Pt wire counter electrode and Pt pseudo reference electrode in acetonitrile with $TBAPF_6$ as the supporting electrolyte and referenced vs Fc/Fc^+.

X. Digestion/Excision Experiment

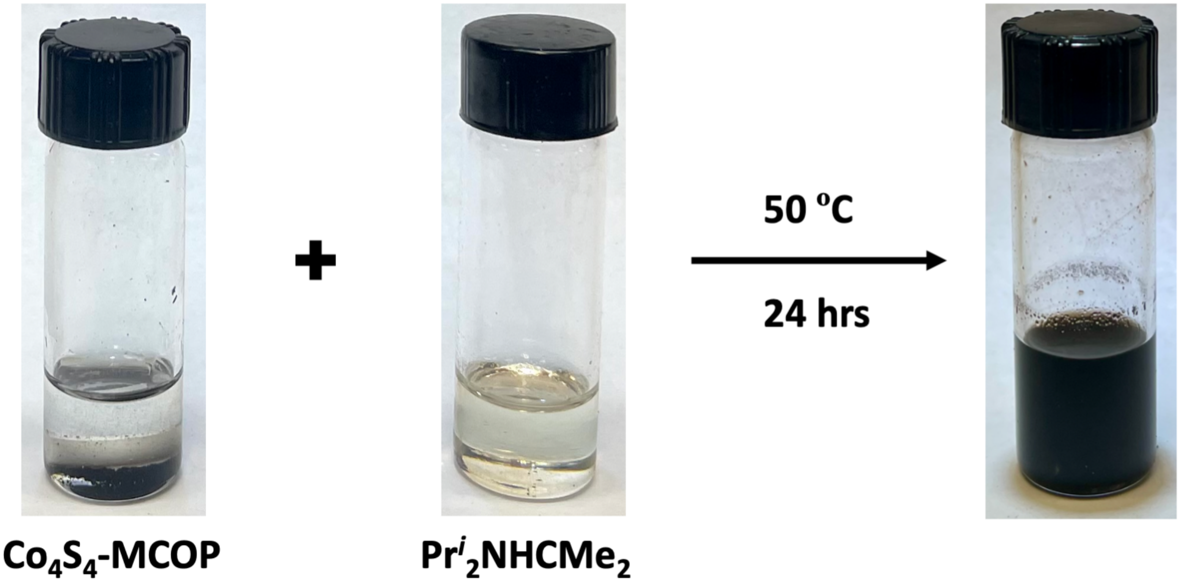

Figure S16. Images from digestion experiment. Suspension of Co_4S_4-MCOP and $Pr^i{}_2$NHCMe$_2$ (20 equivalents) in C_6D_6 were mixed and heated for 50 °C for 24 hours.

XI. SEM Micrographs of Modulated Polymerization

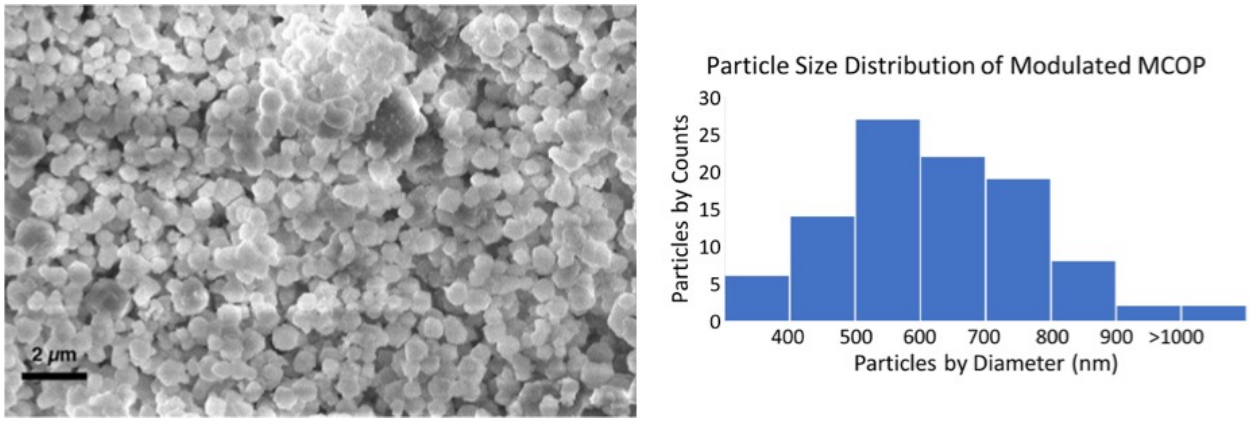

Figure S17. SEM micrograph from modulated synthesis of Co_4S_4-MCOP using 10 equivalents of $Pr^i{}_2$NHCMe$_2$ as a coordination modulator in toluene and particle size distribution histogram as calculated from a sample size of 100 using ImageJ.[3]

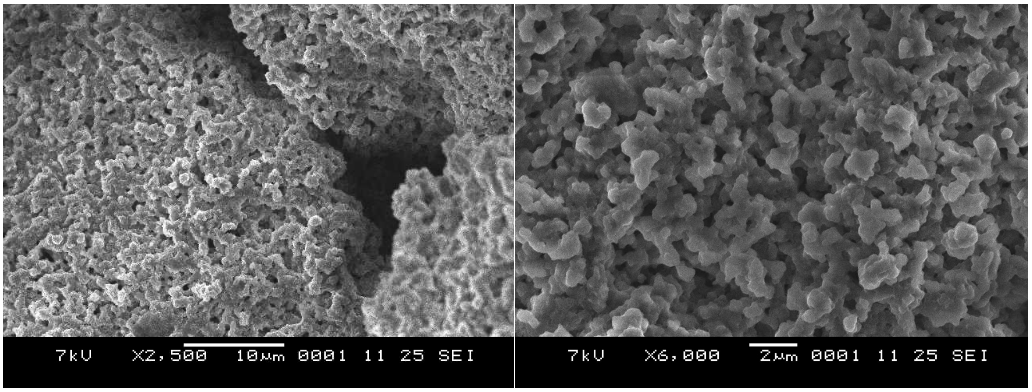

Figure S18. SEM micrographs from modulated synthesis of Co_4S_4-MCOP using 10 equivalents of $Pr^i_2NHCMe_2$ as a coordination modulator in dioxane.

XII. Pre and Post Cyclic Voltammetry SEM/EDS Study

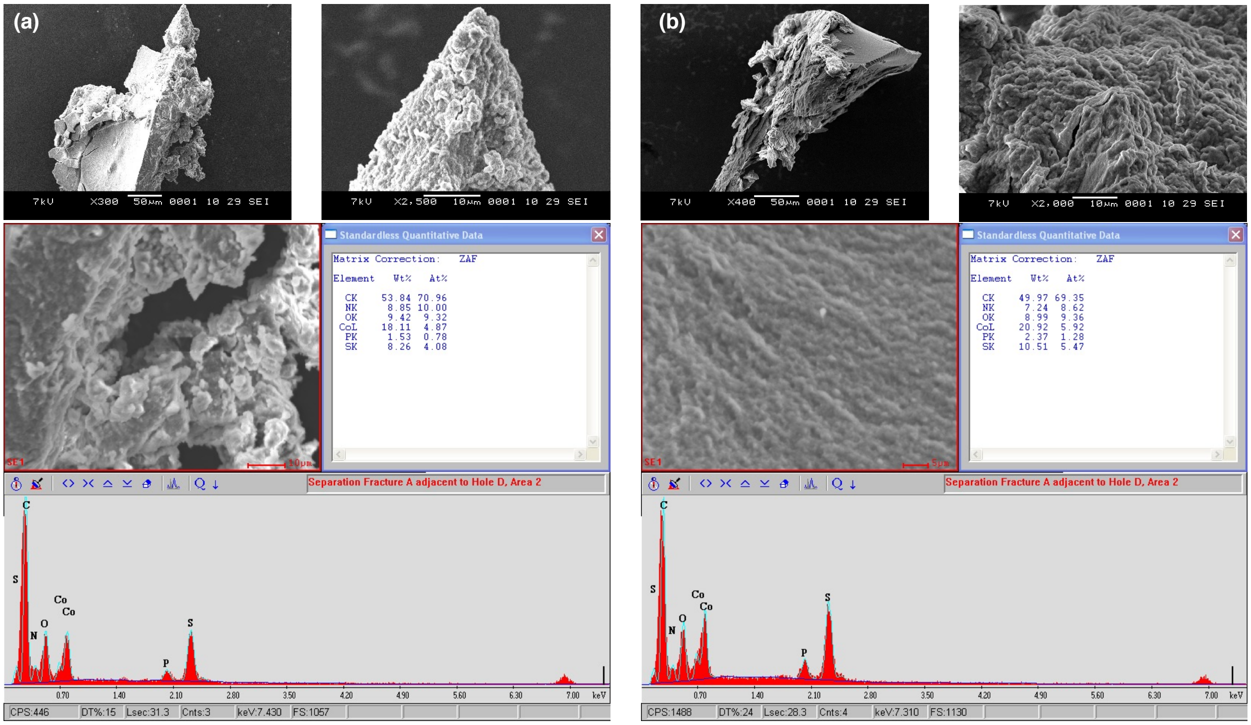

```
Matrix Correction:   ZAF

Element   Wt%   At%

  CK     53.84 70.96
  NK      8.85 10.00
  OK      9.42  9.32
 CoL     18.11  4.87
  PK      1.53  0.78
  SK      8.26  4.08
```

```
Matrix Correction:   ZAF

Element   Wt%   At%

  CK     49.97 69.35
  NK      7.24  8.62
  OK      8.99  9.36
 CoL     20.92  5.92
  PK      2.37  1.28
  SK     10.51  5.47
```

Figure S19. (a) SEM micrographs and EDS scans of Co_4S_4-MCOP before cyclic voltammetry

XIII. Characterization of Co_4S_4-MCOP-Et

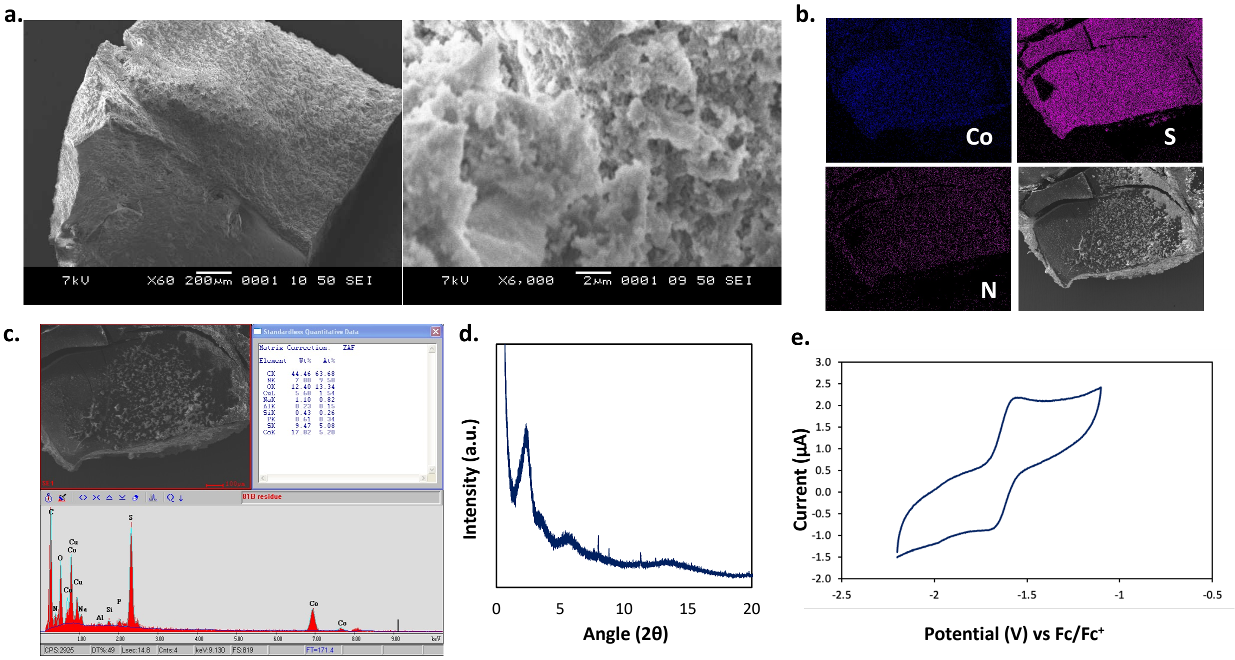

```
Matrix Correction:   ZAF

Element   Wt%   At%

  CK    44.46 63.68
  NK     7.80  9.58
  OK    12.40 13.34
 CuL     5.68  1.54
 NaK     1.10  0.82
 AlK     0.23  0.15
 SiK     0.43  0.26
  PK     0.61  0.34
  SK     9.47  5.08
 CoK    17.82  5.20
```

Figure S20. Characterization of Co_4S_4-MCOP-Et. SEM micrographs (a); EDS mapping (b); EDS scans and elemental composition (c); PXRD pattern (d); solid-state cyclic voltammetry of polymer-modified glassy carbon working electrode, Pt counter electrode, and Pt pseudo reference electrode at a scan rate of 100 mVs^{-1} in a solution of acetonitrile with $TBAPF_6$ as the supporting electrolyte and referenced vs Fc/Fc^+.

XIV. X-ray Diffraction Procedures and Tables

X-ray diffraction data were collected using an Agilent/Oxford Diffraction Gemini A Ultra diffractometer. The diffractometer was equipped with a sealed-tube Mo source with a graphite monochromator (λ=0.71073 Å) and a sealed-tube Cu source with graphite focusing optics (λ=1.54184 Å). In all cases data were collected to better than 0.8 Å resolution.

The CrysAlisPro diffractometer software[4] provided intensity data corrected for Lorentz, polarization, and absorption effects. Preliminary structure solutions were found with the AutoChem software package[4]. Final structures were solved with SHELXT[5] (direct methods) and refined with SHELXL[6], using the Olex2 software package[7]. Anisotropic refinement for all non-hydrogen atoms was performed. Hydrogen atoms were placed in calculated positions. Compound $[Co_4S_4(Pr^i{}_2NHCBz)_4]$ was refined using a solvent mask applied using BYPASS[8]. Using the solvent mask, 45 electrons were found in a volume of 445 $Å^4$ in 2 voids per unit cell. This is consistent with the presence of $0.5[C_4H_{10}O_1]$ per Asymmetric Unit which account for 42 electrons per unit cell.

Publication tables and graphics were generated with the WinGX suite of programs. [9]

Table 1 Crystal data and structure refinement for biscarbene 4.

Identification code	ac_cb_c20h30n4_cu
Empirical formula	$C_{20}H_{30}N_4$
Formula weight	326.48
Temperature/K	101(2)
Crystal system	monoclinic
Space group	$P2_1/c$
a/Å	8.7820(3)
b/Å	9.2791(3)
c/Å	11.5020(5)
α/°	90
β/°	94.287(3)
γ/°	90
Volume/Å^3	934.66(6)
Z	2
ρ_{calc}g/cm^3	1.160
μ/mm^{-1}	0.537
F(000)	356.0
Crystal size/mm^3	0.18 × 0.085 × 0.051
Radiation	Cu Kα (λ = 1.54184)
2Θ range for data collection/°	10.1 to 133.722
Index ranges	$-10 \le h \le 9$, $-10 \le k \le 11$, $-13 \le l \le 13$
Reflections collected	8721
Independent reflections	1655 [R_{int} = 0.0514, R_{sigma} = 0.0323]
Data/restraints/parameters	1655/0/113
Goodness-of-fit on F^2	1.052
Final R indexes [I>=2σ (I)]	R_1 = 0.0394, wR_2 = 0.0922
Final R indexes [all data]	R_1 = 0.0544, wR_2 = 0.1017
Largest diff. peak/hole / e Å^{-3}	0.14/-0.20

Table 2 Crystal data and structure refinement for [$Co_4S_4(Pr^i_2NHCBz)_4$].

Identification code	g2-50
Empirical formula	$C_{52}H_{72}Co_4N_8S_4$
Formula weight	1173.13
Temperature/K	100.00(10)
Crystal system	triclinic
Space group	P-1
a/Å	12.9073(5)
b/Å	13.2862(5)
c/Å	17.5673(6)
α/°	94.342(3)
β/°	95.063(3)
γ/°	93.514(3)
Volume/Å^3	2985.22(19)
Z	2
ρ_{calc}g/cm^3	1.305
μ/mm^{-1}	1.271
F(000)	1224.0
Crystal size/mm^3	0.481 × 0.318 × 0.145
Radiation	Mo Kα (λ = 0.71073)
2Θ range for data collection/°	6.74 to 57.264
Index ranges	$-16 \le h \le 16$, $-16 \le k \le 17$, $-22 \le l \le 22$
Reflections collected	59734
Independent reflections	13795 [R_{int} = 0.0580, R_{sigma} = 0.0620]
Data/restraints/parameters	13795/0/629
Goodness-of-fit on F^2	1.028
Final R indexes [I>=2σ (I)]	R_1 = 0.0416, wR_2 = 0.0813
Final R indexes [all data]	R_1 = 0.0695, wR_2 = 0.0958
Largest diff. peak/hole / e Å^{-3}	0.72/-0.40

XV. References

1. O. V. Starikova, G. V. Dolgushin, L. I. Larina, T. N. Komarova and V. A. Lopyrev, *Arkivoc*, 2003, **2003**, 119–124.

2. H. V. Huynh, Y. Han, J. H. H. Ho and G. K. Tan, *Organometallics*, 2006, **25**, 3267–3274.

3. Rasband, W.S.., ImageJ, U.S. National Institutes of Health, Bethesda, Maryland, USA, https://imagej.nih.gov/ij/, 1997-2018

4. Rigaku Oxford Diffraction, CrysAlisPro Software system, version 1.171.38.46, Rigaku Corporation, Oxford, UK. (2018).

5. G. M. Sheldrick, *Acta Cryst.* C17, 112-122 (2015).

6. G. M. Sheldrick, *Acta Cryst.* A64, 112-122 (2008).

7. Dolomanov, O.V.; Bourhis, L.J.; Gildea, R.J.; Howard, J.A.K.; Puschmann, H., OLEX2: A complete structure solution, refinement and analysis program. J. Appl. Cryst., 42, 339-341 (2009).

8. van der Sluis, P.; Spek, A. L. *Acta Crystallographica Section A* **1990**, *46* (3), 194–201.

9. L. J. Farrugia, *J. Appl. Cryst.* 45, 849-854. (2012)